SLAC–PUB–6043
January 1993
T

α-Helix Propensities of Nonpolar Amino Acids Predicted by Monte Carlo Simulated Annealing*

YUKO OKAMOTO†

Stanford Linear Accelerator Center
Stanford University, Stanford, California 94309

Submitted to *Biopolymers*

---

* Work supported by the Department of Energy, contract DE–AC03–76SF00515.
† On leave of absence from Department of Physics, Nara Women's University, Nara 630, Japan.

ABSTRACT

Monte Carlo simulated annealing is applied to the study of α-helix propensities of seven nonpolar amino acids, Ala, Leu, Met, Phe, Ile, Val, and Gly. Homopolymers of 10 amino acids are used and the propensity is calculated by folding α-helicies from completely random initial conformations. The results suggest the large differences in propensities between helix former and breaker in agreement with the recent experiments with short peptides. It is argued that enthalpy difference for helix-coil transitions will play a major role in determining the helix propensity. The β-strand propensities of the same homopolymers are also considered, and they are shown to agree with the frequencies of amino acids in β-strands.

INTRODUCTION

Recent experimental measurements[1-8] of the α-helix propensities of amino acids in short peptide systems have given a new view of α-helix formation (for a recent review, see Ref. 9). These new experiments suggest large differences in helix propensities among the amino acids, while the conventional view based on the host-guest method[10] indicates small differences. This discrepancy is the motivation for the present work.

A number of techniques have been employed to study the properties of the α-helix theoretically: normal mode calculation,[11,12] harmonic dynamics in dihedral space,[13] unfolding thermodynamics,[14] Monte Carlo simulation,[15-18] molecular dynamics,[21-25] and so on. The major problem in traditional protein simulations such as molecular dynamics lies in the fact that simulations at temperatures of experimental interest (around 0° C) tend to get trapped in one of a huge number of local minima of potential energy. Hence, the simulations strongly depend on the initial conditions, and this is why most simulations start from an ideal helical conformation and the unfolding of the helical conformation is studied. Even unfolding is a difficult task and usually it is studied at high temperatures, such as 327° C [20] and 200° C,[25] where thermal fluctuations are large.

Simulated annealing[26] alleviates this difficulty of dependence on initial conditions, and even *folding* of helices from completely random conformations is possible. The algorithm is based on simulating the process of forming a crystal. By starting a simulation at a sufficiently high temperature (melting), we lower the temperature gradually until the system reaches the global minimum of the potential energy function (crystallization). The final conformation obtained is expected to be close to the native structure. Simulated annealing was applied to crystallographic refinement of protein structures.[27-29] Its application to *ab initio* prediction of peptide and protein conformations was also proposed.[30-32] It was shown that folding of the α-helix from a completely random initial conformation is indeed possible for various polypeptides which are empirically expected to be helical.[33-37]

We remark that simulated annealing also predicts β-strands to be the dominant motif in the peptide fragment BPTI[16-36], which exhibits a β-sheet structure in its natural environment.[38]

In this article, we study α-helix propensities of nonpolar amino acids by Monte Carlo simulated annealing. This is a rerun of Ref. 36, where helix propensities of amino acid homopolymers for Met, Lys, Ser, Tyr, and Gly (all neutral residues) were studied. High helix propensities for Met and Lys and low propensities for Tyr and Gly were predicted in agreement with amino acid frequencies from the protein data base.[39] In the present work we study homopolymers of Ala, Leu, Met, Phe, Ile, Val, and Gly. These amino acids were chosen because new experimental data are available[1-8] and because the effects of solvent will be much smaller than for other (polar) amino acids. The latter point is important, since our simulations neglect solvent molecules. The helix propensities are directly measured by counting the number and length of α-helices obtained and are compared with the empirical data. Energy distributions for helical and non-helical conformations are also analyzed for each homopolymer. Finally, the propensities for β-strand are studied and compared with amino acid frequencies from the protein data base.

METHODS

The homopolymers of seven different nonpolar amino acids, Ala, Leu, Met, Phe, Ile, Val, and Gly, were studied. Each homopolymer had the length of 10 amino acids. Although a longer length is preferred, we chose this length to save computation time. We remark that in our previous work with homopolymers we did not detect much differences in helix propensities between lengths 10 and 15, while the propensities were systematically lower for length 5.[36] Since the charges at peptide termini are known to affect helix propensity,[40,41] we removed them by taking a neutral NH_2– group at the N-terminus and a neutral –COOH group at the C-terminus. The semi-empirical potential energy function that we used is given by the sum of the electrostatic term, 12-6 Lennard-Jones term, hydrogen-bond term, and torsion term with their parameters adopted from ECEPP/2.[42-44]

The computer code KONF90[34,35] was used for Monte Carlo simulated annealing simulations. One Monte Carlo step consists of successively updating all the dihedral angles in the backbone and sidechains. One Monte Carlo simulated annealing run consists of 10^4 Monte Carlo steps with the initial temperature of 1000 K and the final temperature of 250 K with exponential temperature decrease.[34,35] However, the final temperature of 278 K was also considered for homo-alanine in order to examine the dependence on the final temperature. The peptide-bond dihedral angles ω were fixed at 180° for simplicity and the dielectric constant was fixed at $\epsilon = 2$. Twenty runs were made for each homopolymer with completely random initial conformations. The CPU time for one run of homo-Glycine was $\approx$ 18 minutes on IBM9021.

RESULTS AND DISCUSSION

α-Helix Propensities

In order to analyze the α-helix propensities, we adopt the same criterion for α-helix as that defined in Ref. 35; we consider that a residue is in the α-helix state when the dihedral angles (ϕ, ψ) fall in the range $(-60 \pm 45°, -50 \pm 45°)$ in the dihedral space. The *helicity* n is then defined by the number of successive residues which are in the α-helix state. Note that $n = 3$ corresponds to roughly one turn of the α-helix . We consider a conformation as helical if it has a segment with helicity $n \geq 3$.

By examining all the 160 final conformations obtained, we found that no conformation had more than one helical part, i.e., disjoint helices. This is presumably due to the short length, 10, of the homopolymer. We remark that two helices did occur within one peptide conformation when the homopolymer length was 15.[36] Hence, in the present work we have either a non-helical conformation (all $n < 3$) or a helical conformation in which there is only one n satisfying $n \geq 3$ and the rest of n (if they exist) satisfy $n < 3$.

In Table I we summarize the helical content of all the runs. The first entry is the classification of helical conformations in terms of helicity n (≥ 3), or helical

length. We see that $(Met)_{10}$, $(Ala)_{10}$, and $(Leu)_{10}$ gave many helical conformations, 16, 10, and 9 (out of 20), respectively. In particular, Met and Ala produced long helices, some conformations being entirely helical ($n \geq 8$). In Figure 1 we show the "time history" of one run of $(Met)_{10}$; starting from a completely random initial structure (Figure 1(a)), the conformation ends up in an entirely helical structure (Figure 1(f)). We consider that Met, Ala, and Leu are "helix formers". On the other hand, $(Val)_{10}$, $(Ile)_{10}$, and $(Gly)_{10}$ gave few helical conformations, 4, 3, and 2 (out of 20), respectively. Note that we obtained not only a smaller number of helices but also shorter helices than for Met, Ala, and Leu. We conclude that Val, Ile, and Gly are "helix breakers". Finally, the results for $(Phe)_{10}$ indicate that Phe is in-between a helix former and breaker.

The next entry in Table I is the average helicity $< n >_H$ which is an average over only helical segments ($n \geq 3$), and the third entry is the average fraction of residues in the α-helix state, $\frac{<n>}{N}$ ($N = 10$), averaged over the first 10 conformations ($\frac{<n>_{10}}{N}$) and over all 20 conformations ($\frac{<n>_{20}}{N}$). Both $\frac{<n>_{10}}{N}$ and $\frac{<n>_{20}}{N}$ are listed to give a rough estimate of errors. Their difference is the largest, 0.05, for $(Met)_{10}$. Even by taking a conservative value of 0.1 for errors, the differences in $\frac{<n>}{N}$ between helix formers (Met, Ala, and Leu) and helix breakers (Val, Ile, and Gly) are significant.

Let us now consider the rank order of helix propensity for the seven amino acids. From the values of $\frac{<n>_{20}}{N}$, we have

$$\text{Met} > \text{Ala} > \text{Leu} > \text{Phe} > \text{Val} > \text{Ile} > \text{Gly} . \qquad (1)$$

Here, we reversed Phe and Val by considering the significant difference in $< n >_H$, since the longer the helical segment is, the harder it is to form by simulation. That is, when $\frac{<n>_{20}}{N}$ do not differ significantly but $< n >_H$ do between two homopolymers, we considered the amino acid with more $< n >_H$ to be more helix-forming. This rank order (1) can be compared with the experimentally determined helix

propagation parameter s_0 from the host-guest method[10] and s_1[1,5,9] and s_2[4,6] from short peptide systems. These s-values are listed in Table I. It can also be compared with the Chou-Fasman index of helix preference, $P_{\alpha 1}$[39,45] and $P_{\alpha 2}$[46] determined from protein data base. Our rank order (1) agrees qualitatively with the ones given by these emperimental data. In particular, the significant difference in propensity between the helix formers (Met, Ala, and Leu) and helix breakers (Val, Ile, and Gly), which was deduced from our simulations, is evident in all the experimental data except for s_0 of the host-guest method. In other words, our data support the s-values, s_1 and s_2, determined by the recent experimental works on oligopeptides. However, within each group, our results give a slightly different rank order. Namely, Met is the strongest helix former in agreement with s_0 and $P_{\alpha 2}$, but in disagreement with the rest of the experimental data. The propensity of Val is higher than that of Ile, while the experimental data all suggest the opposite. However, these are minor details compared to the propensity differences between helix formers and breakers.

Two more comments regarding Table I are in order. One is that $(\mathrm{Ala})_{10}$ and $(\mathrm{Ala})_{10}^{278}$, where the latter is the results with the final temperature $T = 278$ K instead of 250 K, give a similar helix propensity. $(\mathrm{Ala})_{10}^{278}$ has more $\frac{<n>}{N}$ but less $< n >_H$, compared with $(\mathrm{Ala})_{10}$. Their differences, however, are not so significant as to reverse the rank order with other amino acids. The other point is that the lowest-energy conformation for each homopolymer (marked by a circle in Table I) tends to have the longest helical segment except for Gly. This point will be elaborated more in the next subsection.

Energy Distributions

In this subsection we try to analyze the relation between helix propensity and energy distribution. In Table II we list the ECEPP energy E and helicity $n(n \geq 3)$ for the five lowest-energy conformations of the seven homopolymers. For the helix formers (Met, Ala, and Leu), it is clear that longer helices are energetically favored. This trend is less obvious for the helix breakers (Val, Ile, and Gly), but

the tendency seems to persist, in the sense that even though it is hard to form a helix for this group, helical conformations tend to have low energies once they are formed. The energy difference between helical and non-helical conformations is further elucidated by the histograms of Figure 2. As is clear from the Figure, helical conformations tend to populate the lower-energy bins of the histograms. The difference between helix formers and breakers is that populations are almost divided into two for helix formers: helical group (lower energy) and non-helical group (higher energy), while the energy difference between helical and non-helical conformations is small for the helix breakers. This point is further clarified in Table III where we display the energy difference, $\Delta(E_{min})$, between the minimum energies for non-helical ($E_{min}(NH)$) and helical ($E_{min}(H)$) conformations. We find that $\Delta(E_{min})$ is over 10 kcal/mol for helix formers, while it is less than ≈ 2 kcal/mol for helix breakers. Taking $E_{min}(H)$ for ideal helix (with helicity $n \geq 8$), $\Delta(E_{min})$ for helix breaker slightly increases to ≈ 5 kcal/mol. Since the energy fluctuation around $T = 250$ K is several kcal/mol (data not shown), the energy difference $\Delta(E_{min})$ for helix breakers can be overcome by the entropy effect, while that for helix formers cannot.

β-Strand Propensities

In this subsection we analyze the propensities of β-strand formation. For this we consider that a residue is in β-strand state when the dihedral angles (ϕ, ψ) fall in the range $(-130 \pm 50°, 135 \pm 45°)$ in the dihedral space. The *strand tendency* m is then defined by the number of successive residues which are in the β-strand state. We consider a conformation as a strand if its strand tendency m is ≥ 3.

In Table IV we summarize the results together with the Chou-Fasman index of β-strand preference, $P_{\beta 1}$[39,45] and $P_{\beta 2}$.[46] Even though the results are not as obvious as in the α-helix case, we can deduce the rank order of strand propensity for the seven amino acids. By taking into account both $\frac{<m>}{N}$ and $< m >_S$, we have

$$\text{Val} > \text{Ile} > \text{Phe} > \text{Leu} > \text{Ala} > \text{Met} > \text{Gly} . \qquad (2)$$

This is in reasonable agreement with $P_{\beta 1}$ and $P_{\beta 2}$. By comparing this with (1), we find that the helix-forming group is the strand-breaking group and vice versa, except for Gly. Gly is both helix and strand breaking. The reason is probably because Gly has a much larger (dihedral) conformation space than the rest of the amino acids.

CONCLUSIONS

In this article we have studied the α-helix propensities of nonpolar amino acids, Ala, Leu, Met, Phe, Ile, Val, and Gly, by Monte Carlo simulated annealing. The outstanding characteristic of the present work lies in the fact that we study direct *folding* of helices from completely random initial conformations in a bias-free manner. The results support the conclusions of new experiments with short peptides[1-9] rather than those of the host-guest model[10] in that helix formers (Ala, Leu, and Met) have substantially larger helix propensities than substantially larger propensity than helix breakers (Ile, Val, and Gly).

These propensity differences between helix formers and breakers are interpreted as resulting from enthalpy differences ΔH between helical and non-helical states. Namely, for the helix breakers ΔH is small and the entropy term is important, while for the helix formers the helix state is favored by the significant ΔH.

Acknowledgements:

The auther would like to thank Professor Baldwin of Stanford University School of Medicine for many helpful discussions and suggestions and critical reading of the manuscript. He is also grateful to the members of Baldwin Group and Stanford Linear Accelerator Center for their kind hospitality.

REFERENCES

1. Padamanabhan, S., Marqusee, S., Ridgeway, T., Laue, T.M. & Baldwin, R.L. (1990) *Nature* **344**, 268–270.

2. Merutka, G., Lipton, W., Shalango, W., Park, S.-H. & Stellwagen, E. (1990) *Biochemistry* **29**, 7511–7515.

3. O'Neil, K.T. & DeGrado, W.F. (1990) *Science* **250**, 646–651.

4. Lyu, P.C., Liff, M.I., Marky, L.A. & Kallenbach, N.R. (1990) *Science* **250**, 669–673.

5. Chakrabartty, A., Schellman, J.A. & Baldwin, R.L. (1991) *Nature* **351**, 586–588.

6. Gans, P.J., Lyu, P.C., Manning, M.C., Woody, R.W. & Kallenback, N.R. (1991) *Biopolymers* **31**, 1605–1614.

7. Kemp, D.S., Boyd, J.G. & Muendel, C.C. (1991) *Nature* **352**, 451–454.

8. Stellwagen, E., Park, S.-H., Shalango, W. & Jain, A. (1992) *Biopolymers* **32**, 1193–1200.

9. Chakrabartty, A. & Baldwin, R.L. (1992) in *Protein Folding: In Vivo and In Vitro*, Cleland, J. & King, J., Eds., ACS Press, in press.

10. Sueki, M., Lee, S., Power, S.P., Denton, J.B., Konishi, Y. & Scheraga, H.A. (1984) *Macromolecules* **17**, 148–155.

11. Fanconi, B., Small, E.W. & Peticolas, W.L. (1971) *Biopolymers* **18**, 2465–2495.

12. Levy, R.M. & Karplus, M. (1979) *Biopolymers* **18**, 2465–2495.

13. Gō, M. & Gō, N. (1976) *Biopolymers* **15**, 1119–1127.

14. Ooi, T. & Oobatake, M. (1991) *Proc. Natl. Acad. Sci. U.S.A.*, **88**, 2859–2863.

15. Skvortsov, A.M., Birshtein, T.M. & Zalenski, A.O. (1971) *Mol. Biol.* **5**, 69.

16. Ripoll, D.R. & Scheraga, H.A. (1988) *Biopolymers* **27**, 1283–1303.

17. Vila, J., Williams, R.L., Grant, J.A., Wójcik, J. & Scheraga, H.A. (1992) *Proc. Natl. Acad. Sci. U.S.A.*, **89**, 7821–7825.

18. Creamer, T.P. & Rose, G.D. (1992) *Proc. Natl. Acad. Sci. U.S.A.*, **89**, 5937–5941.

19. Levy, R.M., Perahia, D. & Karplus, M. (1982) *Proc. Natl. Acad. Sci. U.S.A.*, **79**, 1346–1350.

20. Brooks, B.R. (1989) *Chem. Scripta* **29A**, 165–169.

21. Tirado-Rives, J. & Jorgensen, W.L. (1991) *Biochemistry* **30**, 3864–3871.

22. Daggett, V., Kollman, P.A. & Kuntz, I.D. (1991) *Biopolymers* **31**, 1115–1134.

23. Soman, K.V., Karimi, A. & Case, D.A. (1991) *Biopolymers* **31**, 1351–1361.

24. Hermans, J., Anderson, A.G. & Yun, R.H. (1992) *Biochemistry* **31**, 5646–5653.

25. Daggett, V. & Levitt, M. (1992) *J. Mol. Biol.* **223**, 1121–1138.

26. Kirkpatrick, S., Gelatt, C.D., Jr. & Vecchi, M.P. (1983) *Science* **220**, 671–680.

27. Nilges, M., Clore, G.M. & Gronenborn, A.M. (1988) *FEBS Lett.* **229**, 317–324.

28. Brünger, A.T. (1988) *J. Mol. Biol.* **203**, 803–816.

29. Brünger, A.T., Karplus, M. & Petsko, G.A. (1989) *Acta Cryst.* A**45**, 50–61.

30. Wilson, S.R., Cui, W., Moskowitz, J.W. & Schmidt, K.E. (1988) *Tetrahedron Lett.* **29**, 4373–4376.

31. Kawai, H., Kikuchi, T. & Okamoto, Y. (1989) *Protein Eng.* **3**, 85–94.

32. Wilson, C. & Doniach, S. (1989) *Proteins* **6**, 193–209.

33. Wilson, S.R. & Cui, W. (1990) *Biopolymers* **29**, 225–235.

34. Kawai, H., Okamoto, Y., Fukugita, M., Nakazawa, T. & Kikuchi, T. (1991) *Chem. Lett.* **1991**, 213–216.

35. Okamoto, Y., Fukugita, M., Nakazawa, T. & Kawai, H. (1991) *Protein Eng.* **4**, 639–647.

36. Fukugita, M., Nakazawa, T., Kawai, H. & Okamoto, Y. (1991) *Chem. Lett.* **1991**, 1279–1282.

37. Okamoto, Y., Kikuchi, T., Nakazawa, T. & Kawai, H. (1992) "Prediction of Tertiary Structure of Parathyroid Hormone Fragment (1-34) by Monte Carlo Simulated Annealing", Nara Women's University preprint NWU-7/92, submitted for publication.

38. Nakazawa, T., Kawai, H., Okamoto, Y. & Fukugita, M. (1992) *Protein Eng.* **5**, 495–503.

39. Chou, P.Y. and Fasman, G.D. (1974) *Biochemistry* **13**, 222–245.

40. Ihara, S., Ooi, T. & Takahashi, S. (1982) *Biopolymers* **21**, 131–145.

41. Shoemaker, K.R., Kims, P.S., York, E.J., Stewart, J.M. & Baldwin, R.L. (1987) *Nature* **326**, 563–567.

42. Momany, F.A., McGuire, R.F., Burgess, A.W. & Scheraga, H.A. (1975) *J. Phys. Chem.* **79**, 2361–2381..

43. Némethy, G., Pottle, M.S. & Scheraga, H.A. (1983) *J. Phys. Chem.* **87**, 1883–1887.

44. Sippl, M.J., Némethy, G. & Scheraga, H.A. (1984) *J. Phys. Chem.* **88**, 6231–6233.

45. Chou, P.Y. (1979) in *CECAM Protein Folding Workshop*, Universite de Paris-Sud, Orsay, France, p.p. 149–216.

46. Levitt, M. (1978) *Biochemistry* **17**, 4277-4285.

Table I. α-Helix Formation of Homopolymers in 20 Monte Carlo Simulated Annealing Runs[a]

Peptide	$(Met)_{10}$	$(Ala)_{10}$	$(Leu)_{10}$	$(Phe)_{10}$	$(Val)_{10}$	$(Ile)_{10}$	$(Gly)_{10}$	$(Ala)_{10}^{278}$
n								
3	1	0	3	1	1	(3)	2	3
4	3	1	2	2	(3)	0	0	2
5	0	1	1	1	0	0	0	1
6	2	2	(3)	0	0	0	0	1
7	1	2	0	(1)	0	0	0	3
8	(6)	(2)	0	0	0	0	0	(3)
9	2	2	0	0	0	0	0	1
10	1	0	0	0	0	0	0	0
Total	16/20	10/20	9/20	5/20	4/20	3/20	2/20	14/20
$< n >_H$	6.9	6.9	4.4	4.6	3.8	3.0	3.0	5.9
$\frac{<n>_{10}}{N}$	0.70	0.47	0.42	0.23	0.27	0.20	0.11	0.55
$\frac{<n>_{20}}{N}$	0.65	0.46	0.41	0.23	0.28	0.17	0.14	0.58
s_0	1.20	1.07	1.14	1.09	0.95	1.14	0.59	
s_1	0.87	1.99	1.70		0.20	0.44	0.02	
s_2	1.41	2.19	1.55		0.93	1.02	0.57	
$P_{\alpha 1}$	1.32	1.39	1.30	1.11	0.97	0.99	0.63	
$P_{\alpha 2}$	1.47	1.29	1.30	1.07	0.91	0.97	0.56	

[a] $(Ala)_{10}^{278}$ stands for the simulation with the final temperature of 278 K, and the rest are the simulation with the final temperature of 250 K. The first entry is the number of helical conformations (i.e., conformations with *helicity* $n \geq 3$). A number in a circle indicates that one of the conformations in that entry is the lowest-energy structure in the 20 Monte Carlo runs for the corresponding homopolymer. See text for the definition of other entries.

Table II. ECEPP Energy E (kcal/mol) and *Helicity* n ($n \geq 3$) of Five Lowest-Energy Conformations in 20 Monte Carlo Simulated Annealing Runs[a]

	$(Met)_{10}$		$(Ala)_{10}$		$(Leu)_{10}$		$(Phe)_{10}$		$(Val)_{10}$		$(Ile)_{10}$		$(Gly)_{10}$	
	E	n	E	n	E	n	E	n	E	n	E	n	E	n
1	−28.8	8	−2.8	8	−12.5	6	−50.9	7	17.8	4	34.5	3	−3.2	
2	−25.0	9	−2.3	8	−7.1	6	−48.8	5	18.3		36.1		−0.1	
3	−23.5	8	−1.5	9	−1.1	4	−47.3	4	19.0	4	38.2		0.0	3
4	−22.9	8	1.2	6	2.9	3	−46.9		19.5		38.7	3	0.0	
5	−21.3	8	1.3	9	3.9	4	−45.0	3	19.9		41.3	3	1.6	

[a] The relative energy differences among homopolymers are meaningless.

Table III. Energy Differences between the Minima of Non-Helican and Helical Conformations[a]

Peptide	$(Met)_{10}$	$(Ala)_{10}$	$(Leu)_{10}$	$(Phe)_{10}$	$(Val)_{10}$	$(Ile)_{10}$	$(Gly)_{10}$
$E_{min}(NH)$	−12.6	8.3	9.0	−46.9	18.3	36.1	−3.2
$E_{min}(H)$	−28.8	−2.8	−12.5	−50.9	17.8	34.5	0.0
$\Delta(E_{min})$	16.2	11.1	21.5	4.0	0.5	1.6	−3.2

[a] $\Delta(E_{min}) \equiv E_{min}(NH) - E_{min}(H)$.

Table IV. β-Strand Formation of Homopolymers in 20 Monte Carlo Simulated Annealing Runs[a]

Peptide	$(Met)_{10}$	$(Ala)_{10}$	$(Leu)_{10}$	$(Phe)_{10}$	$(Val)_{10}$	$(Ile)_{10}$	$(Gly)_{10}$	$(Ala)_{10}^{278}$
m								
3	0	0	2	5	1	(7)	0	0
4	0	0	0	1	0	4	0	0
5	0	0	0	0	2	1	0	0
6	0	0	0	0	1	0	0	0
7	0	0	0	0	0	0	0	0
8	0	0	0	0	1	0	0	0
9	0	0	0	0	0	0	0	0
10	0	0	0	0	0	0	0	0
Total	0/20	0/20	2/20	6/20	5/20	12/20	0/20	0/20
$< m >_S$	0.0	0.0	3.0	3.2	5.4	3.5	0.0	0.0
$\frac{<m>_{10}}{N}$	0.08	0.18	0.22	0.27	0.39	0.43	0.03	0.12
$\frac{<m>_{20}}{N}$	0.09	0.17	0.22	0.33	0.41	0.43	0.04	0.10
$P_{\beta 1}$	1.01	0.79	1.17	1.23	1.64	1.57	0.87	
$P_{\beta 2}$	0.97	0.90	1.02	1.32	1.49	1.45	0.92	

[a] Each entry corresponds to that of Table I with *helicity* n replaced by *strand tendency* m. See text and Table I for the definition of the corresponding entries.

FIGURE CAPTIONS

1) Backbone structure of $(Met)_{10}$ from a run which ended up in an entirely helical conformation: the initial structure (a), at 2000 Monte Carlo (MC) step (b), at 4000 MC step (c), at 6000 MC step (d), at 8000 MC step (e), and the final structure (f).

2) Histogram of energy distributions for helical conformations (solid bars) and non-helical conformations (shaded bars): $(Met)_{10}$ (a), $(Ala)_{10}$ (b), $(Leu)_{10}$ (c), $(Phe)_{10}$ (d), $(Val)_{10}$ (e), $(Ile)_{10}$ (f), and $(Gly)_{10}$ (g). The energy differences in absolute values among homopolymers are meaningless.

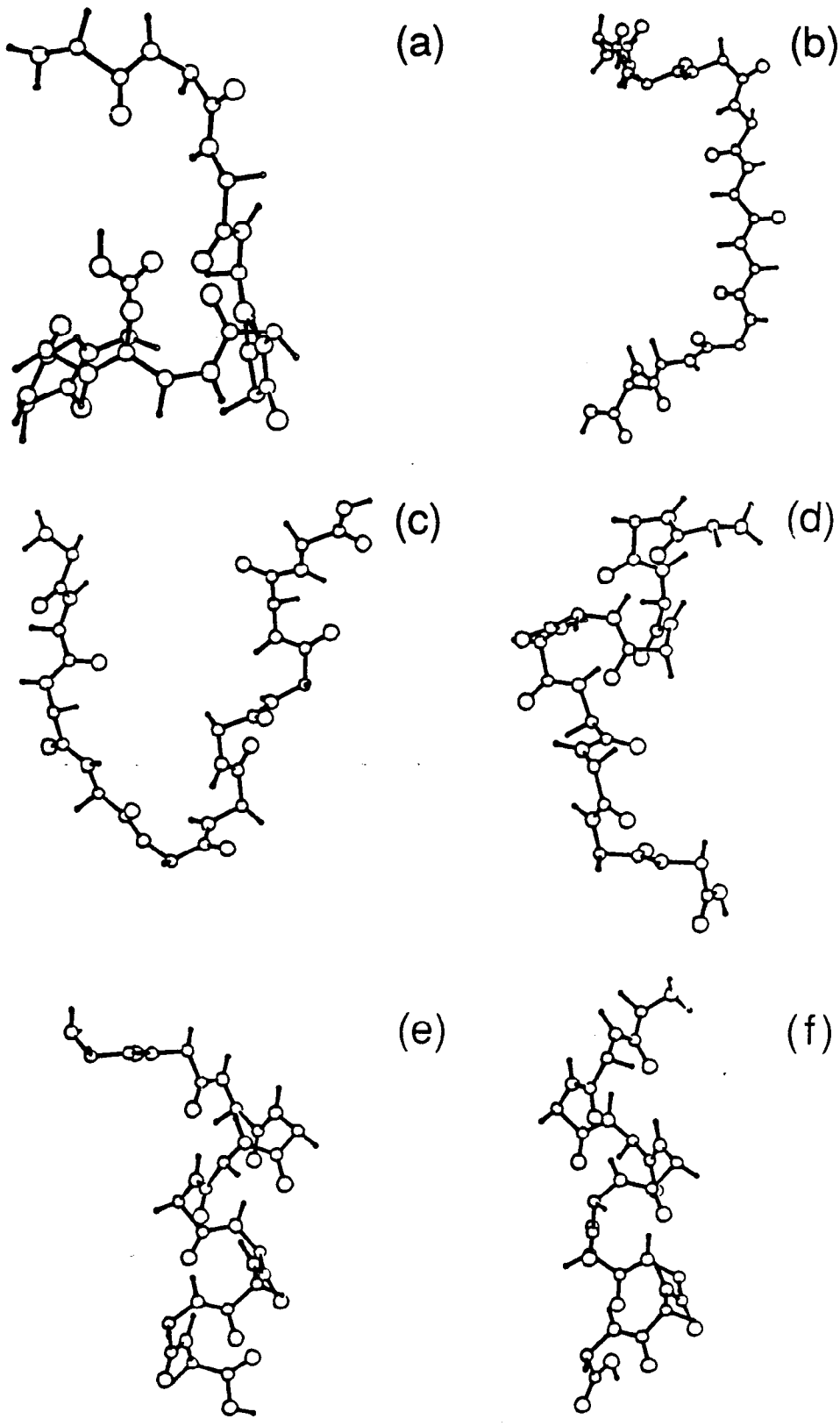

Fig. 1

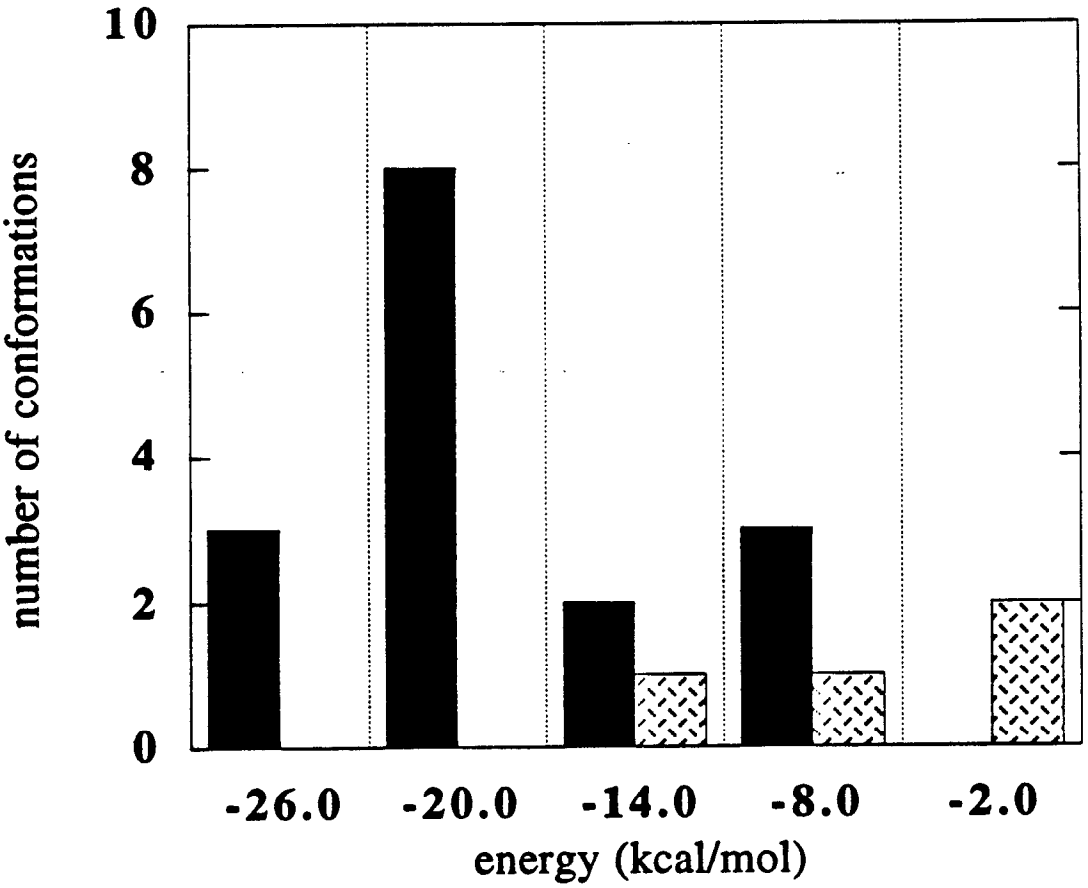
10
8
6
4
2
0
number of conformations
-26.0
-20.0
-14.0
-8.0
-2.0
energy (kcal/mol)

Fig. 2(a)

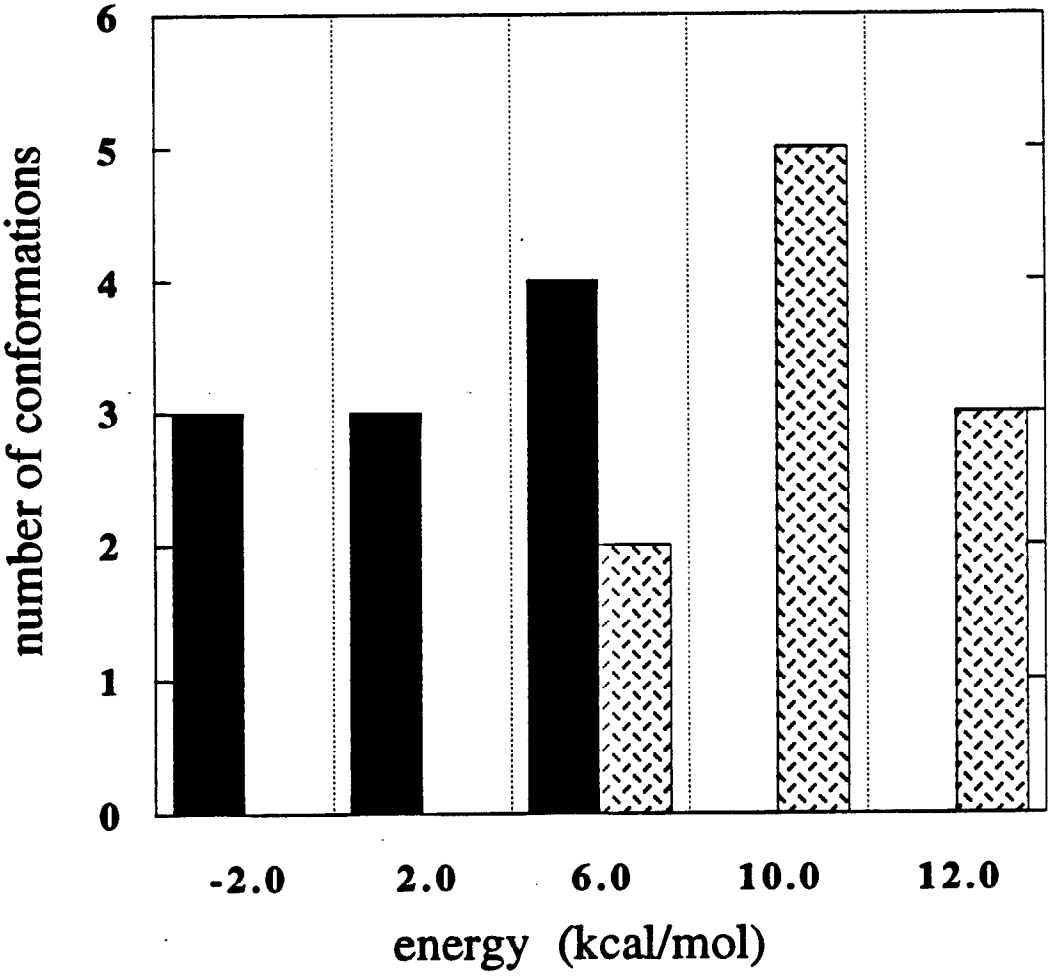
number of conformations
6
5
4
3
2
1
0
-2.0
2.0
6.0
10.0
12.0
energy (kcal/mol)

Fig. 2(b)

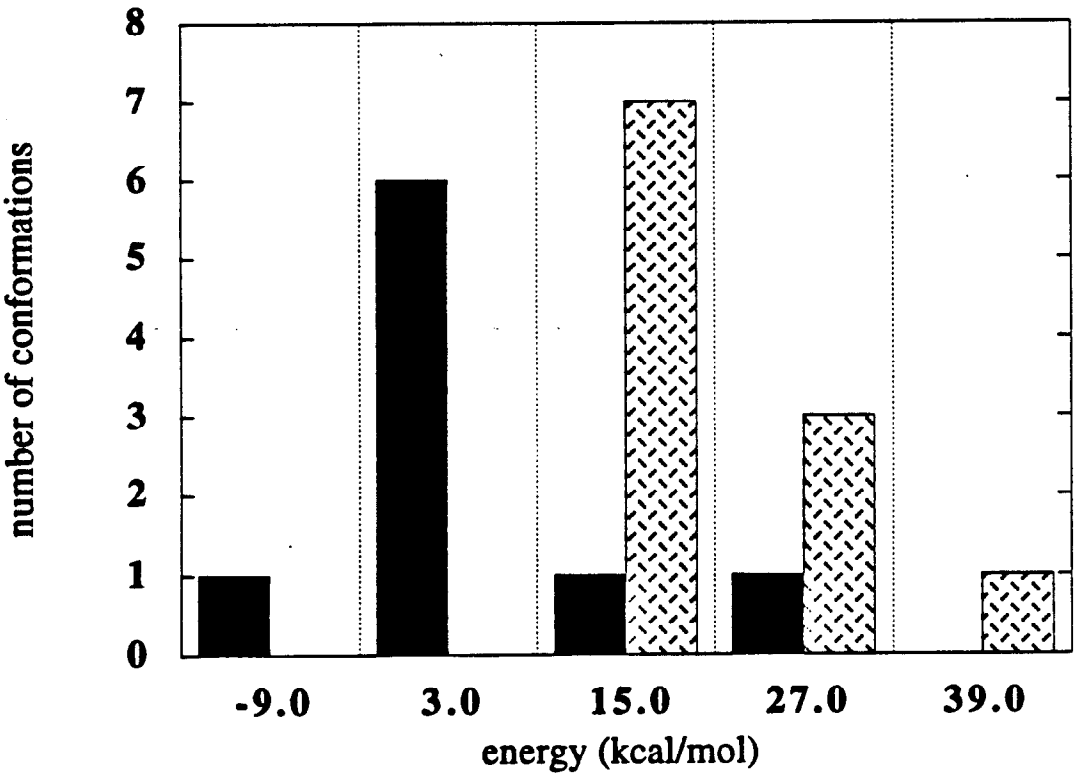
number of conformations
8
7
6
5
4
3
2
1
0
-9.0
3.0
15.0
27.0
39.0
energy (kcal/mol)

Fig. 2(c)

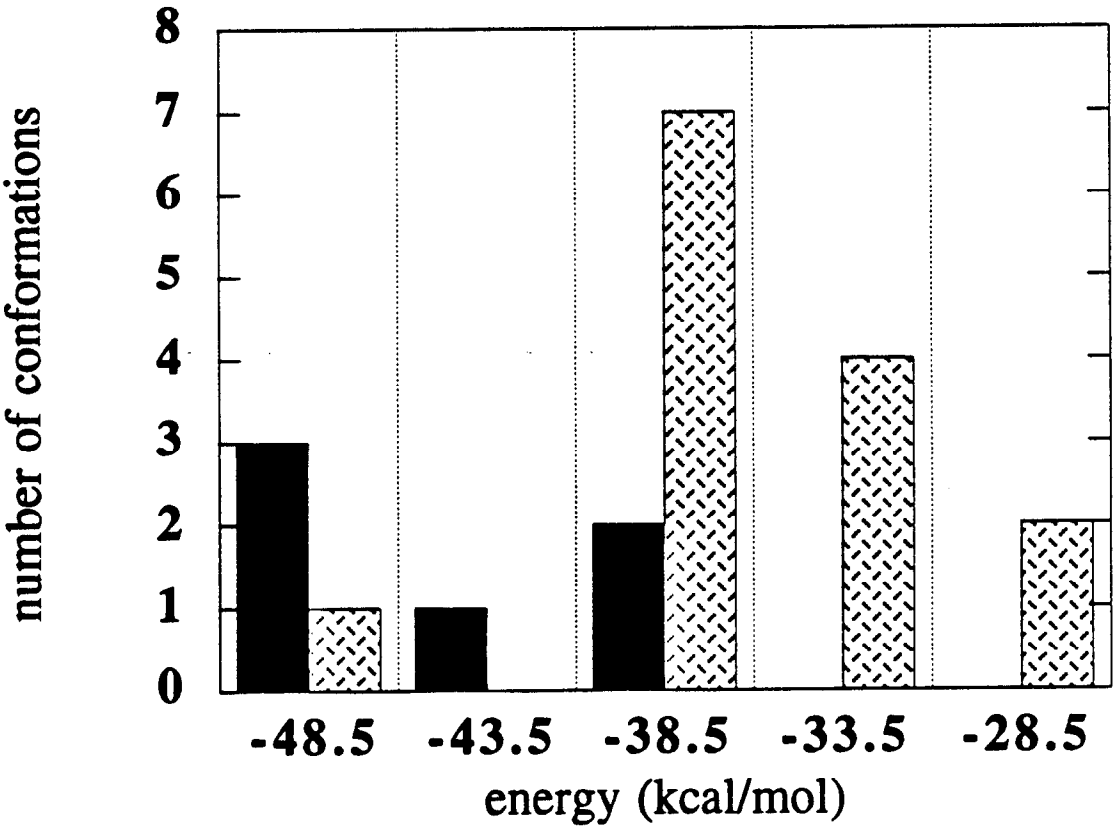
number of conformations
8
7
6
5
4
3
2
1
0
-48.5
-43.5
-38.5
-33.5
-28.5
energy (kcal/mol)

Fig. 2(d)

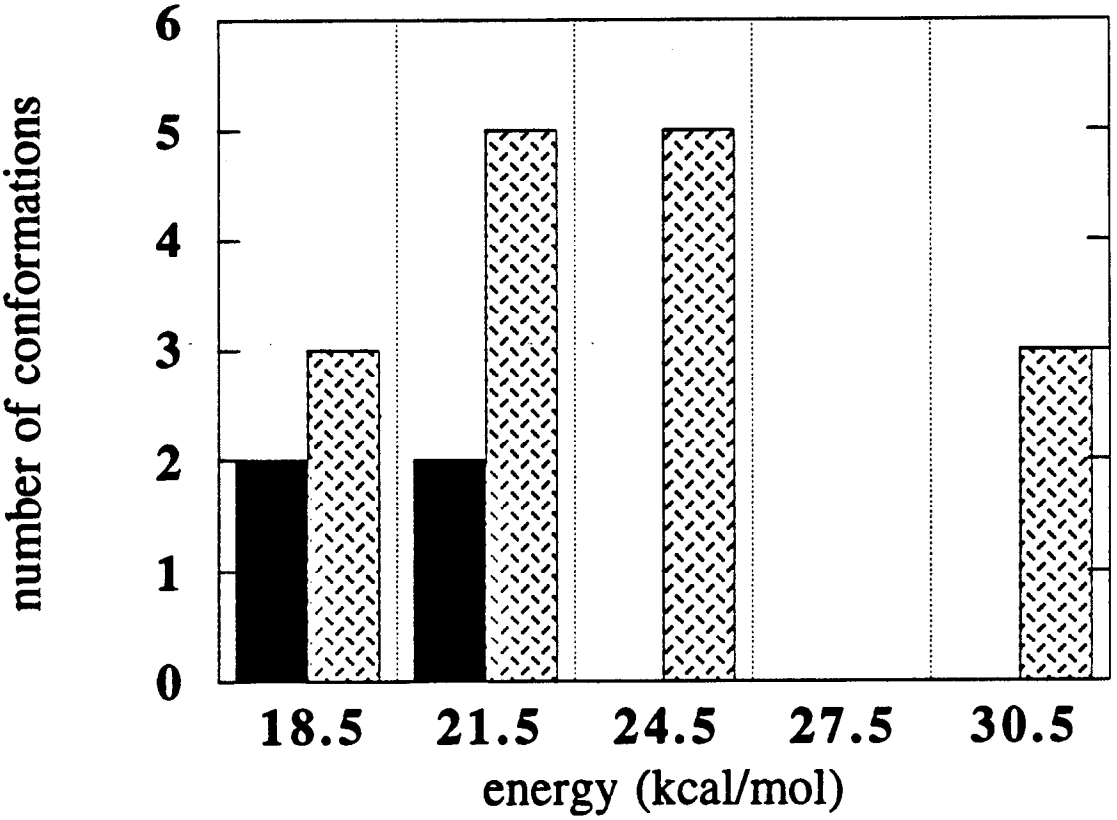
number of conformations
6
5
4
3
2
1
0
18.5
21.5
24.5
27.5
30.5
energy (kcal/mol)

Fig. 2(e)

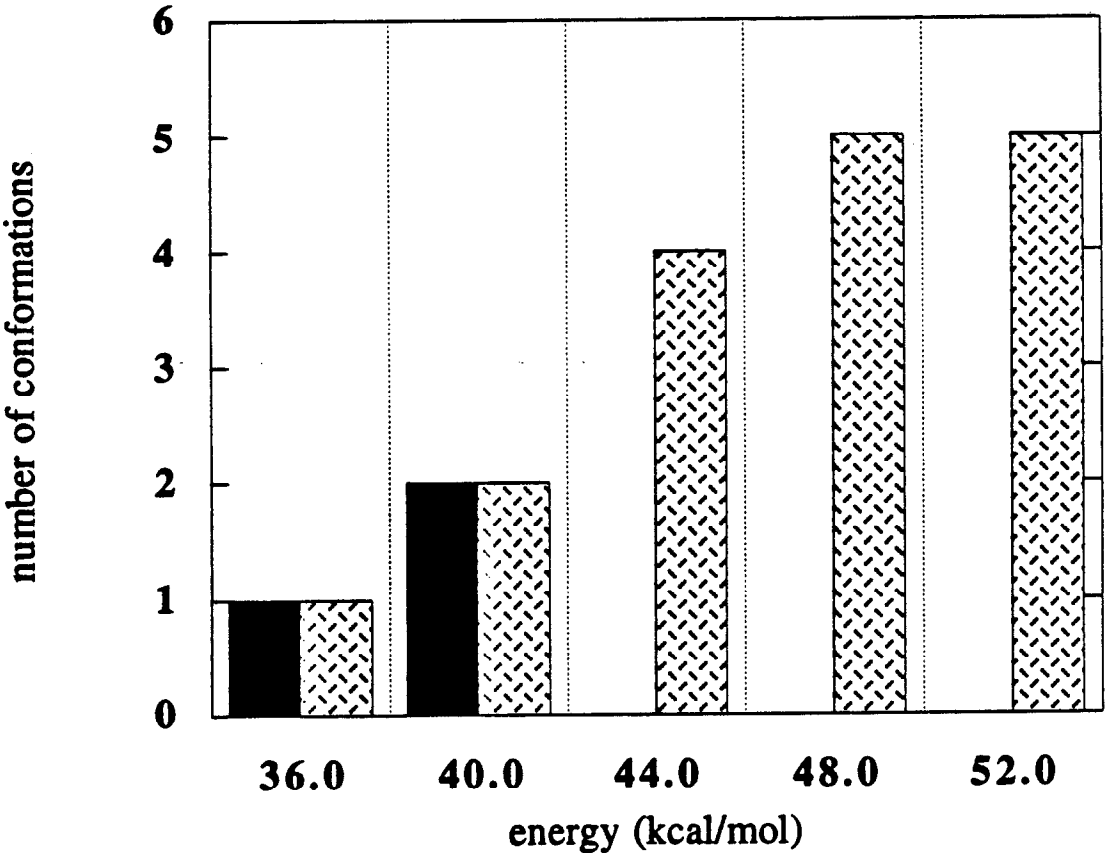
number of conformations
6
5
4
3
2
1
0
36.0
40.0
44.0
48.0
52.0
energy (kcal/mol)

Fig. 2(f)

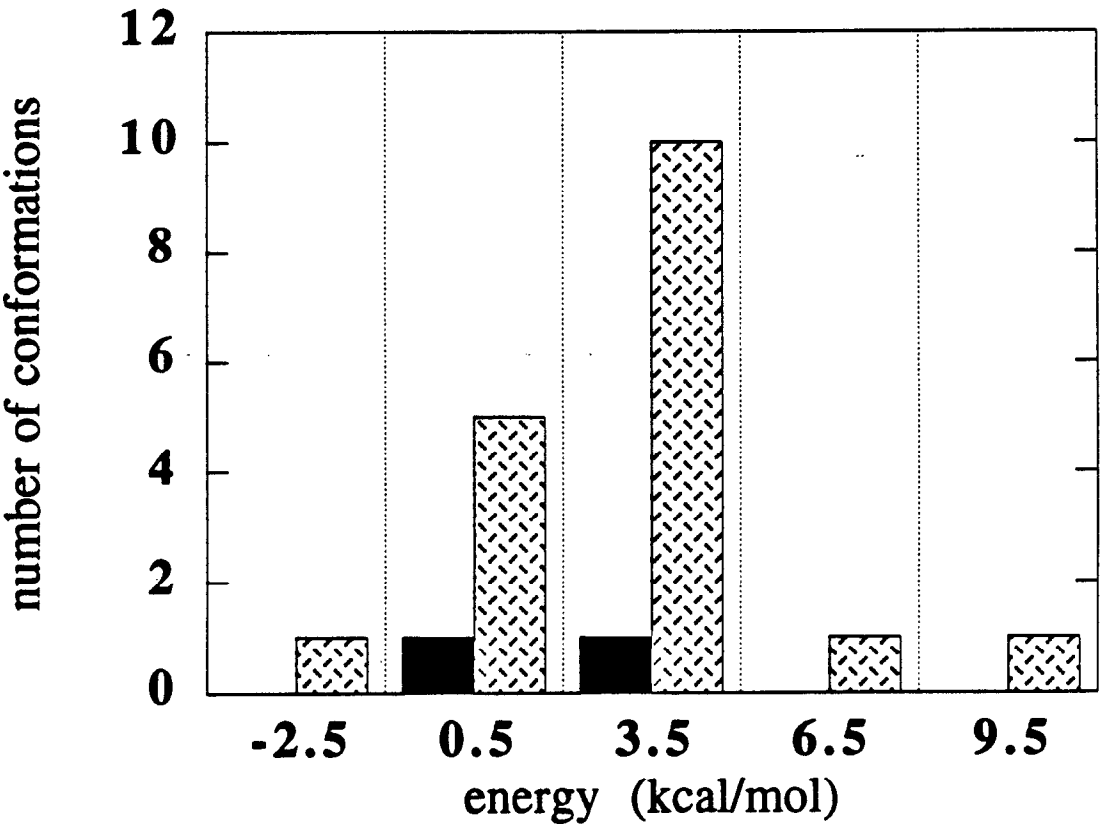
number of conformations
12
10
8
6
4
2
0
-2.5
0.5
3.5
6.5
9.5
energy (kcal/mol)

Fig. 2(g)